Binding of 2-Aryl-4-(piperidin-1-yl)butanamines and 1,3,4-Trisubstituted Pyrrolidines to Human CCR5: A Molecular Modeling-Guided Mutagenesis Study of the Binding Pocket

Laurie A. Castonguay,*,‡ Youmin Weng,§ William Adolfsen,§ Jerry Di Salvo,§ Ruth Kilburn,§ Charles G. Caldwell,|| Bruce L. Daugherty,§ Paul E. Finke,|| Jeffrey J. Hale,|| Christopher L. Lynch,|| Sander G. Mills,|| Malcolm MacCoss,|| Martin S. Springer,§ and Julie A. DeMartino§

Departments of Molecular Systems, Immunology and Rheumatology, and Medicinal Chemistry, Merck Research Laboratories, P.O. Box 2000, Rahway, New Jersey 07065

Received August 14, 2002; Revised Manuscript Received November 27, 2002

ABSTRACT: The results of investigations in these laboratories of 2-aryl-4-(piperidin-1-yl)butanamines and 1,3,4-trisubstituted pyrrolidines as human CCR5 antagonists have recently been disclosed. To facilitate further development of these antagonists, we have developed a pharmacophore model based on the structure−activity relationships (SAR) and a human CCR5 receptor docking model using the crystal structure of rhodopsin as a template [Palczewski, K., et al. (2000) *Science 289*, 739−745]. Guided by the receptor docking model, we have mapped the compounds' site of interaction with CCR5 using site-directed mutagenesis experiments. Our results are consistent with a binding site for the two series that is located within a cavity near the extracellular surface formed by transmembrane helices 2, 3, 6, and 7. This site is overlapping yet distinct from that reported for another antiviral agent which binds to CCR5 [Dragic, T., et al. (2000) *Proc. Natl. Acad. Sci. U.S.A. 97*, 5639−5644].

CCR5, a seven-transmembrane GPCR[1] for the chemokines, MIP-1α, MIP-1*β*, and RANTES, has been identified as an HIV coreceptor, which together with CD4 is used by macrophage-tropic (M-tropic) strains of HIV to infect target cells (*1*−*5*). M-tropic strains initiate the infection and dominate during the asymptomatic stages of the disease. As infection proceeds, T cell-tropic (T-tropic) viruses can emerge which utilize another chemokine receptor, CXCR4, as the coreceptor. The importance of CCR5 for the establishment of the initial infection was demonstrated by human genetic studies of high-risk individuals (*6*). Individuals allelically homo- or heterozygous for a 32 bp deletion in the gene encoding CCR5 exhibit either resistance to HIV-1 infection or delayed progression to frank AIDS, respectively (*7*, *8*). Furthermore, the natural ligands of CCR5, RANTES, MIP-1α, and MIP-1*β*, as well as N-terminally modified forms of RANTES, have been shown to block infection of M-tropic strains (*9*).

Given the importance of CCR5 for the establishment, and possibly maintenance, of HIV-1 infection in vivo, numerous efforts to identify suitable CCR5 antagonists for use as potential anti-HIV-1 therapeutic agents have been initiated. Reports from Takeda (*10*), Schering-Plough (*11*), and Merck (*12*−*16*) describing small molecule human CCR5 receptor antagonists that inhibit HIV replication have recently ap-

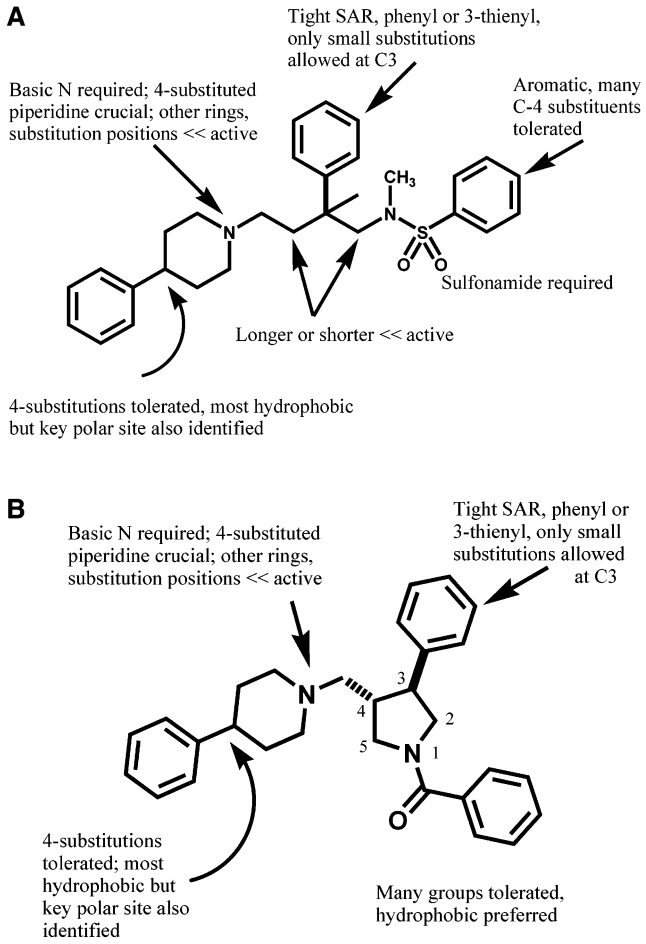

FIGURE 1: General structure−activity relationships for (A) 1-amino-2-phenyl-4-(piperidin-1-yl)butane series and (B) 1,3,4-trisubstituted pyrrolidine series. The pyrrolidine numbering scheme that was used is shown on the ring.

* To whom correspondence should be addressed. Phone: (732) 594-6301. Fax: (732) 594-4224. E-mail: laurie_castonguay@merck.com.
‡ Department of Molecular Systems.
§ Department of Immunology and Rheumatology.
|| Department of Medicinal Chemistry.

[1] Abbreviations: HIV-1, human immunodeficiency virus type 1; ECL, extracellular loop; R5, macrophage-tropic; MIP, macrophage inflammatory protein; RANTES, regulated on activation normal T cell-expressed and -secreted; SAR, structure−activity relationship; GPCR, G protein-coupled receptor.

10.1021/bi026639s CCC: $25.00
Published on Web 01/22/2003

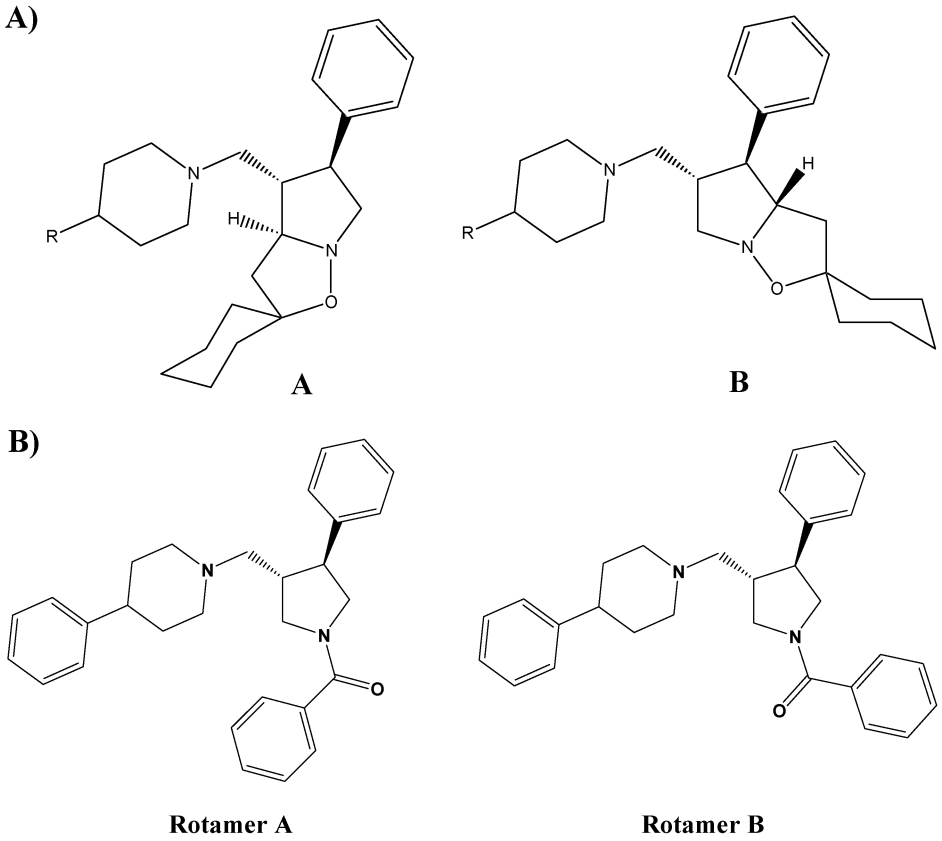

FIGURE 2: Methylenecyclohexane-derived isoxazolidones used to determine the pharmacophore shape shown in panel A. Two possible rotamers for compound **2** are shown in panel B.

peared. An alanine scanning mutagenesis study of CCR5 identified the receptor-binding site of Takeda's dual CCR5 and CCR2b antagonist, TAK-779 (*17*). TAK-779 was reported to bind within a cavity formed by helices 1−3 and 7 near the extracellular surface of CCR5. Herein, we show that the binding site for the Merck compounds is also located near the extracellular surface of CCR5, but primarily within a cavity formed by transmembrane helices 2, 3, 6, and 7.

MATERIALS AND METHODS

Pharmacophore Model. Conformations for all compounds were generated using an in-house distance geometry program (S. K. Kearsley, unpublished results) and energy-minimized using a distance-dependent dielectric constant of 78 and the MMFFs force field (*18*). The pharmacophore model was created by generating a consensus overlay of all compounds using MEGA-SQ (*19*). The final model was chosen on the basis of comparison with the experimental SAR (Figures 1 and 2) and is shown in Figure 3.

CCR5 Receptor Docking Model. A 3D model of the human CCR5 receptor was constructed on the basis of the manual sequence alignment between bovine rhodopsin and human CCR5 (Figure 4). Using the Protein Design module within Quanta2000 (*20*), the homology model was created from this alignment using the coordinates of the bovine rhodopsin crystal structure as the backbone template for the transmembrane helices. The side chain positions were placed using the following procedure. All atoms of the side chain in common with atoms in the template were copied, and those that differed with the template were built according to known side chain preferences. The loop regions were added to the

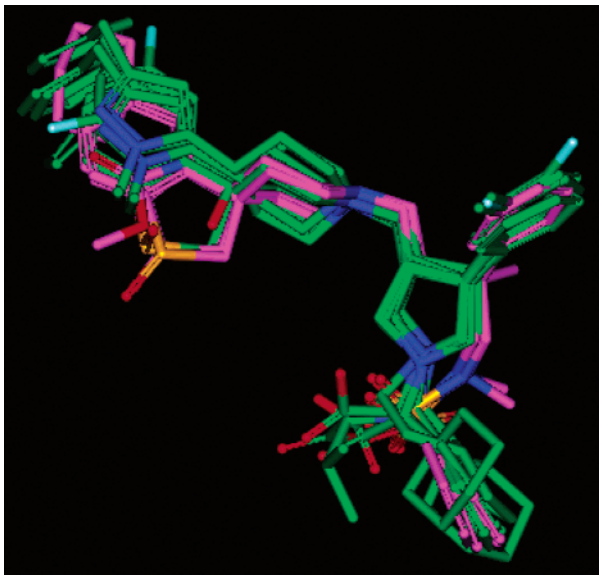

FIGURE 3: Pharmacophore model for CCR5 antagonists. The pyrrolidine series is shown in green and the acyclic series in magenta. The coloring scheme is as follows: green or magenta for carbon, red for oxygen, dark blue for nitrogen, orange for sulfur, and light blue for a heteroatom.

helices by searching a library of protein structures generated from the Protein Data Bank (*21*) for protein fragments that most closely matched the geometric requirement of connecting one helix to the next. The backbone and side chains for these loops were added in a similar manner as in the helices using the closest fragment as the template. The receptor model was then refined using the CHARMm force field (*22*)

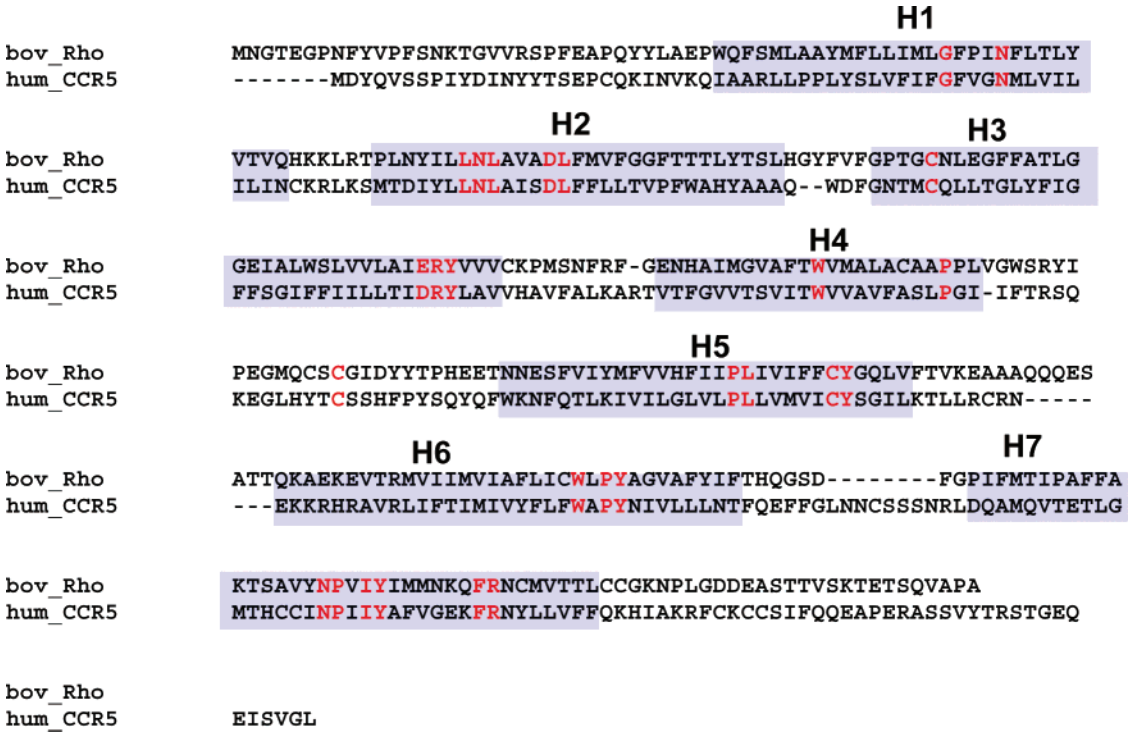

FIGURE 4: Sequence alignment of bovine rhodopsin with human CCR5. The seven transmembrane helices are shown in the blue boxes. The residues shown in red are typical conserved motifs found in many family A GPCRs.

in a stepwise process. First, the backbone of the transmembrane helices was held fixed during 200 steps of steepest descent minimization to remove side chain close contacts. Next, the α-carbons of the transmembrane helices were held fixed, and 1000 steps of molecular dynamics were carried out following 300 steps of heating to 300 K and 300 steps of equilibration. Finally, the resulting model minimized for 200 steps of conjugate gradient minimization with no constraints yielded a model with no close contacts present. A manual docking of the pharmacophore model into the hCCR5 receptor model was then carried out. First, the compounds were placed near the 11-*cis*-retinal chromophore-binding site in the bovine rhodopsin crystal structure (*23*). The SAR and shape versus fit of the pocket versus the pharmacophore shape and characteristics were used to guide the docking. The receptor docking model is shown in Figures 5 and 6.

Materials. All human chemokines were from Peprotech (Rocky Hill, NJ). Radioactive chemokines were from Perkin-Elmer NEN (Boston, MA). ^{35}S-labeled Merck compound **3** was prepared by the in-house Labeled Compound Synthesis group.

Cloning and Mutagenesis of CCR5. Since it was reported that human CCR5 was located within 17 kb of human CCR2 on human chromosome 3p21 (*24*), the human CCR5 open reading frame would most likely be present on a genomic clone carrying CCR2. Accordingly, human CCR5 was cloned by PCR using 10 ng of a human P1 genomic DNA clone previously defined to contain CCR2 (DMPC-HFF No. 1: Clone 785-8C; Genome Systems, Inc., St. Louis, MO) as a template (*25*) with the following primers: 5′-primer, 5′-ATA-TAT-TAA-GCT-TCC-ACC-ATG-GAT-TAT-CAA-GTG-TCA-AGT-C-3′; 3′-primer, 5′-ATA-TAT-TCT-AGA-GCG-GCC-GCT-CAC-AAG-CCC-ACA-GAT-ATT-TC-3′. PCR was carried out with the following cycling parameters (94 °C for 1 min, 55 °C for 1 min, and 72 °C for 2 min) for 30 cycles and a GeneAmp kit (Perkin-Elmer). The resulting PCR product, approximately 1.1 kb in length, was digested with *Hin*dIII and *Xba*I (sites present on the 5′- and 3′-primers, respectively) and cloned into staging vector pSP72 (Promega), and six clones were sequenced. Three clones were found to contain the identical human CCR5 sequence that was reported previously (*24*). CCR5 mutants were prepared with the QuickChange mutagenesis kit (Stratagene, La Jolla, CA), as described by the manufacturer.

Expression of Wild-Type and Mutant CCR5 in CHO Cells. CHO cells (10^6, ATCC CCL-61) were plated in F12 medium supplemented with 10% FBS 16 h prior to being transfected with 20 μg of expression plasmid DNA using a standard calcium phosphate procedure (Specialty Media, Lavallette, NJ) or using Lipofectamine 2000 (Invitrogen). The DNA was incubated with cells at 37 °C in 6% CO_2 for 6 h, whereupon the medium was removed and the cells were glycerol-shocked (for calcium phosphate-transfected cells only, 15% glycerol shock solution, Specialty Media) and refed with medium containing 1.0 mg/mL Geneticin (Invitrogen). After incubation for 10 days, the surviving foci were pooled. Stable expression of CCR5 was verified by determining that an aliquot of these cells bound radiolabeled MIP-1α (see binding parameters below). The remaining cells were cloned by limiting dilution in 96-well microtiter plates, and the cells were expanded. Stable cell lines were derived from individual clones selected on the basis of binding and functional assays. Alternatively for some mutants, cells from pooled foci were used in the binding assays following verification of radiolabeled MIP-1α binding.

Binding Assays. Binding of [^{125}I]RANTES and [^{125}I]MIP-1α (2200 Ci/mmol, typically 20 000 cpm, 20 pM per assay point) in the presence of unlabeled ligands or a serially diluted compound was initiated by adding intact cells

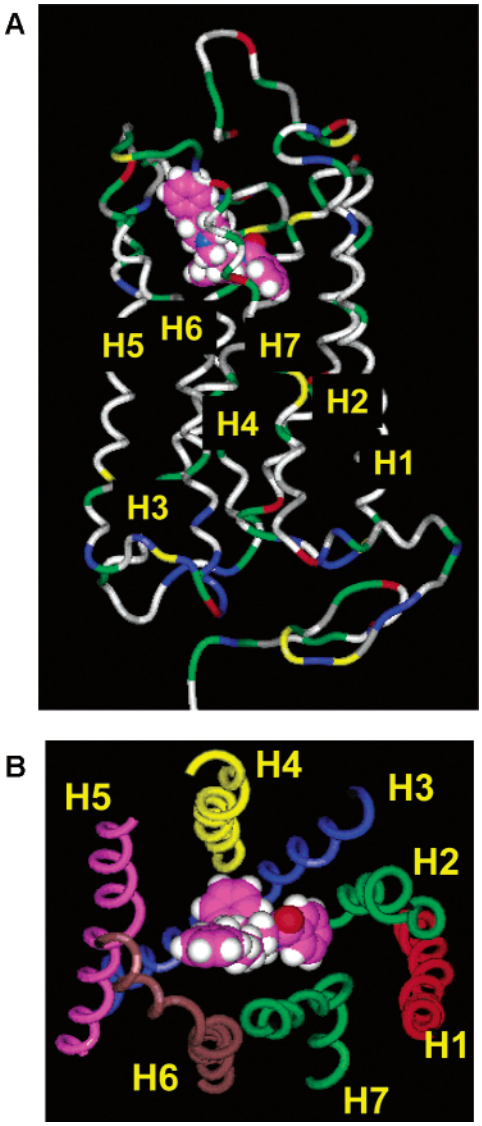

FIGURE 5: (A) Human CCR5 receptor binding model shown with compound **2** docked in the homology model. The residue color scheme for the receptor model is as follows: green for hydrophobic, white for polar, gray for aromatic, yellow for sulfur-containing, red for acidic, and blue for basic. (B) View of the CCR5 receptor docking model from its extracellular surface. The model is rotated approximately 90° from the orientation shown in panel A. All loops have been removed for clarity.

(75000−200000 cells per point) as previously described (*26*). Binding proceeded at room temperature for 60 min, whereupon the assay was terminated by filtering through GF/C filters treated with 0.33% PEI. The filters were then washed two times (500 μL each) with buffer containing 50 mM HEPES (pH 7.2), 0.1% BSA, 0.02% NaN_3, 1 mM $CaCl_2$, 5 mM $MgCl_2$, and 0.5 M NaCl. Binding assays using ^{35}S-labeled compound **3** were performed as described above except that the binding proceeded for 2 h at room temperature and the plates were washed three times with the above wash buffer containing 5% Tween 20 (Sigma). The filters were counted in a standard gamma counter, and the results were analyzed using Graph Pad Prism software.

RESULTS AND DISCUSSION

Extensive screening of the sample collection of Merck Research Laboratories led to the identification of several

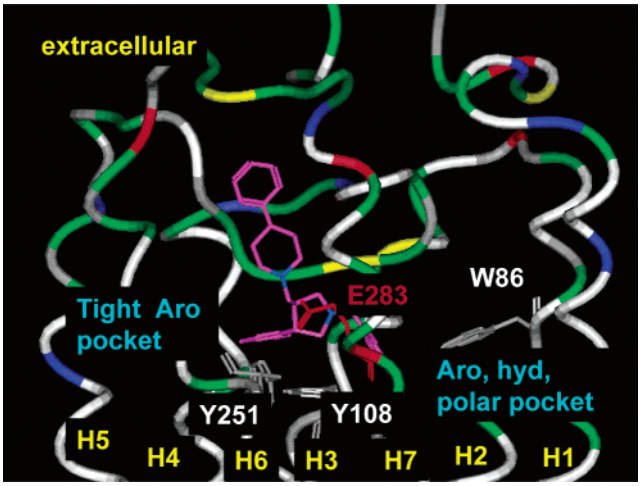

FIGURE 6: Close-up view of the binding model with compound **2**. The color scheme is the same as in Figure 5A.

acyclic 2-aryl-4-(piperidin-1-yl)butanamine analogues as CCR5 antagonists. Subsequently, the development of the SAR around these lead compounds, as well as the 1,3,4-trisubstituted pyrrolidines, has been reported recently (*12*−*16*). Figure 1 summarizes these SARs for receptor binding. In general, the SARs for the pyrrolidine and acyclic series are quite similar with one exception noted below. The 4-substituted piperidine with its basic nitrogen is crucial in both series. Other ring sizes and substitution patterns were found to be much less active. Appropriately substituted polar groups off the 4 position of the piperidine ring were found to be potency-enhancing in both series. In the pyrrolidine series, there is a restricted SAR in the 3-aryl position, and similarly in the 2-aryl position of the acyclic series. This phenyl was found to be important for potency, and substitution was limited to small moieties at the 3 position. There is a significant divergence in the SAR between the two series in the 1 position. In the pyrrolidine series, numerous N-substituents were tolerated, although hydrophobic groups were preferred. In the acyclic series, an aryl sulfonamide was required and 4-substitution off the phenyl group was tolerated.

On the basis of this emerging SAR for the 2-aryl-4-(piperidin-1-yl)butanamine and 1,3,4-trisubstituted pyrrolidine series, a pharmacophore model was developed. Several overlays of multiple compounds from both series were generated. The parallel SAR between the 3-aryl position in the pyrrolidine series and the 2-aryl position in the acyclic series led to the overlap of these aryl groups in the pharmacophore model. The 4-phenyl piperidine ring was overlapped between the two series, consistent with the comparable SAR. Two rotamers were plausible for the N-1 substitution in the pyrrolidine series as shown in Figure 2B. The acyclic series can be matched to either rotamer due to its greater flexibility. An exact overlay of the 1 position is not expected since the SAR for the two series diverges at this point. Bicyclic isoxazolidines, as shown in Figure 2A, were prepared as conformationally constrained N-1 substituted pyrrolidines and provided insight into the stereochemical requirements at this position (*27*). Rotamer B was found to be the preferred geometry for the pyrrolidine series. The final pharmacophore model, shown in Figure 3, was chosen on the basis of an overlay of both series, consistent with

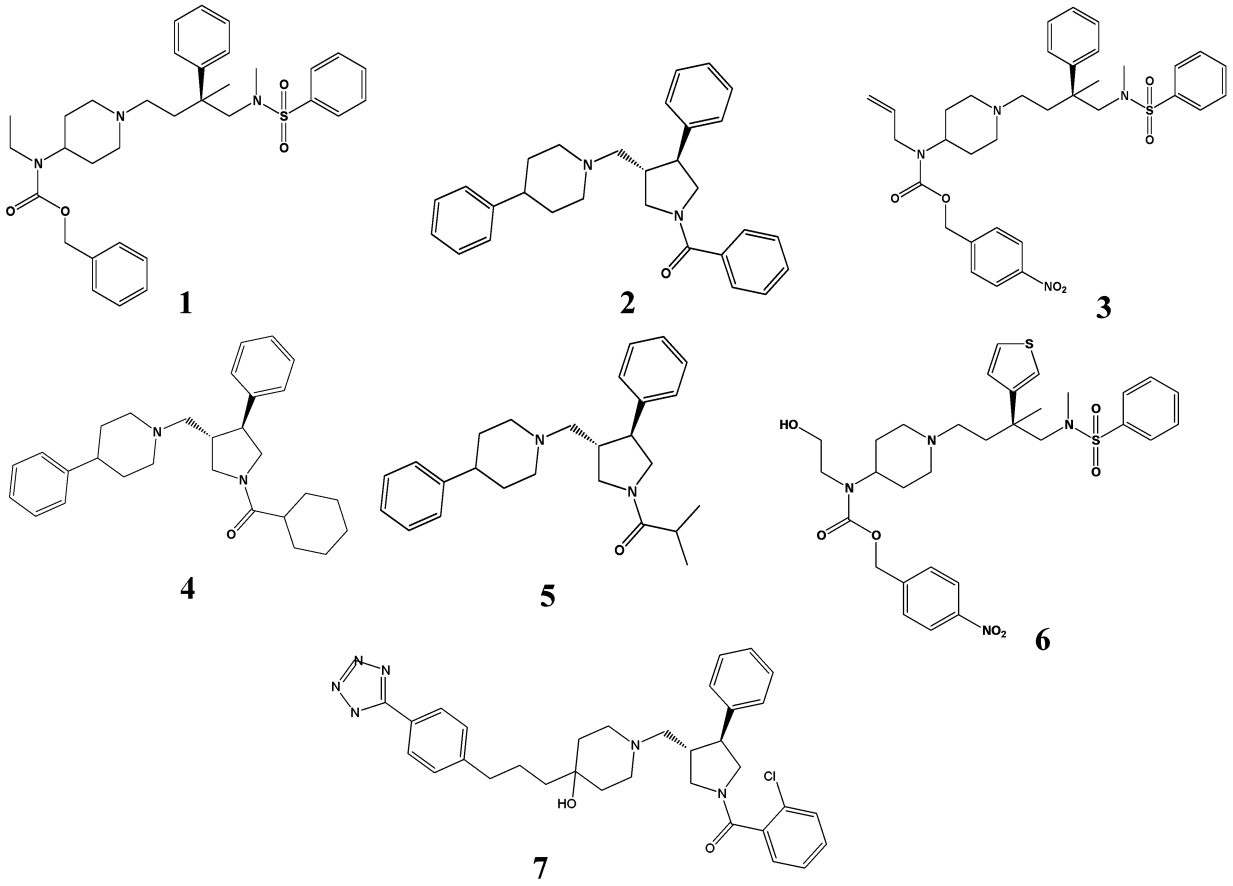

FIGURE 7: CCR5 antagonists.

rotamer B and the overlap of the aryl and piperidine groups as discussed above.

A homology model for the human CCR5 receptor was built using the recently released bovine rhodopsin crystal structure as a template (*23*). The sequence alignment of human CCR5 with bovine rhodopsin that was used is shown in Figure 4. Highlighted in red are the residues that were used to identify the seven transmembrane helices. These are conserved motifs found in most family A GPCRs. An antagonist binding site model was developed by manually docking the pharmacophore model into the CCR5 receptor model. The SAR of the two series and the shape of the pharmacophore model were used to predict the most likely orientation of the compounds in the receptor model. As shown in Figures 5 and 6, the proposed antagonist binding site in CCR5 is located in a pocket near the top of helices 2, 3, 6, and 7.

To test this model, several residues within the receptor were picked for site-directed mutagenesis: Y108 (H3) and Y251 (H6) as well as two acidic residues, D276 (H7) and E283 (H7), which could potentially interact with the required basic amines in the two compound series. Each of the residues was mutated to alanine, and the binding affinities of these modified receptors for a panel of compounds (Figure 7) were tested. MIP-1α and RANTES were used as controls. The mutation results are summarized in Table 1, and a typical competition curve is shown Figure 8A. In general, reduced affinity for the mutated receptors was seen for E283 in helix 7, Y108 in helix 3, and Y251 in helix 6. No significant effect was seen for D276 in helix 7 or the controls MIP-1α and RANTES with any substitution.

Table 1: Mutational Results for Compounds and Controls (nM)[a]

compound	CCR5	D276A	E283A	Y108A	Y251A	Y37A	W86A
1	4.0	23	>1000	1010	110	2.9	210
2	10	16	>10000	165	110	NT[b]	NT[b]
3	1.7	4.0	1000	230	18	1.3	130
4	23	72	>10000	970	280	130	>1000
5	120	350	>10000	3200	9800	180	830
6	2.0	4.0	>10000	750	51	3.3	910
7	11	5.0	>10000	150	55	10	120
MIP-1α	0.65	6.6	1.8	NT[b]	NT[b]	1.1	4.4
RANTES	0.50	8.3	0.91	1.7	0.45	NT[b]	NT[b]

[a] Shown are average values from at least three independent determinations. [b] Not tested.

After the publication of the TAK-779 alanine scanning mutagenesis study, two additional mutants were made, Y37A (H1) and W86A (TM2), since alanine substitutions at these two residues significantly hindered the ability of TAK-779 to inhibit HIV viral entry (*17*). No significant effect on Merck compound binding affinity was seen for Y37A in helix 1, but a reduced affinity was seen for W86A in TM2 (Table 1). Further comparison revealed that while both TAK-779 and the Merck compounds were strongly affected by the Y108A mutation, E283A only moderately affected TAK-779 antiviral activity (*17*), whereas a significantly reduced binding affinity was observed for all the Merck compounds (Table 1). These results suggest that the TAK-779 and the Merck compound binding sites partially overlap, or alternatively, these differences could due to virus and receptor interaction versus compound and receptor binding. To directly determine if TAK-779 and the Merck compound binding sites overlap, competition binding was performed

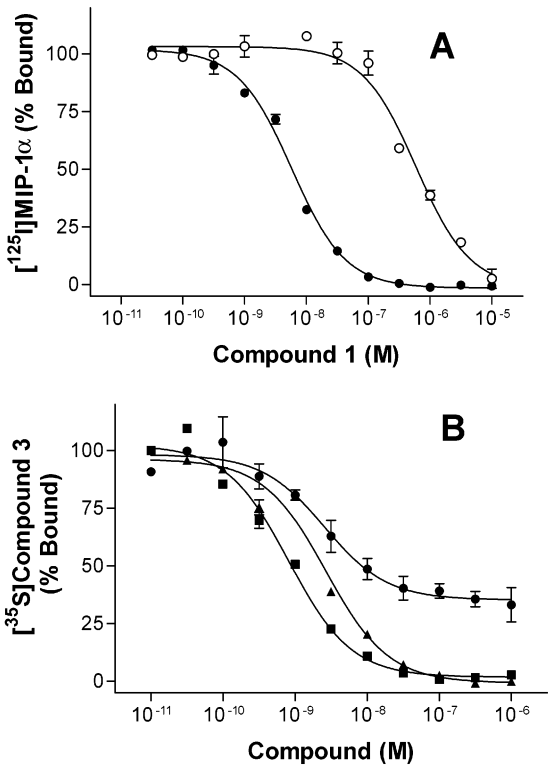

FIGURE 8: (A) Titration of Merck compound **1** in the CCR5 binding assay using the wild-type receptor (●) or the Y108A mutant (○). Data represent means ± the standard deviation of duplicate determinations from a single representative experiment. (B) Titration of TAK-779 (●), compound **1** (▲), and compound **3** (■) using ^{35}S-labeled compound **3** and wild-type CCR5. For data analysis, the counts per minute obtained in the presence of 1 μM compound **3** were used to define maximal inhibition. Data represent means ± the standard deviation of quadruplicate determinations from a single representative experiment.

using labeled Merck compound **3** (Figure 7). TAK-779 only partially inhibited compound **3** binding (Figure 8B), although the observed affinity for CCR5 (2.8 nM) is in agreement with published values (*10*). In contrast, unlabeled compound **3** and compound **1** were able to completely inhibit binding to CCR5. These results are consistent with TAK-779 and the Merck compounds having only partially overlapping binding sites.

As indicated earlier, since the basic nitrogen in the piperidine ring was required, it seemed reasonable to orient the compounds to allow this nitrogen to interact with E283 in helix 7 (Figure 6). This decision was supported by the greatly reduced affinity (81−5000-fold reduction) seen for the E283A mutant receptor. Although D276, also in helix 7, is another potential site of interaction, the lack of an effect of the D276A substitution indicates that this residue plays little role in compound binding.

In the 3-aryl position of the pyrrolidine series, as in the 2-aryl position of the acyclic series, very little substitution is tolerated and an aromatic moiety is required. Therefore, this aryl group was docked in a size-restricted aromatic pocket formed between helix 3 and 6 that contains tyrosines 251 (H6) and 108 (H3). Mutation of Y251 and Y108 to alanine resulted in decreased affinities for all compounds that were tested, although, in general, the reductions were greater for Y108A (14−375-fold) than for Y251A (5−79-fold). This pocket contains several additional aromatic residues, and one can postulate that the compound's placement may shift slightly if interactions are made with these other residues.

The N-1 substituents in the pyrrolidine series and the aryl sulfonamide in the acyclic series are docked into the pocket formed by helices 2, 3, and 7 which contains hydrophobic, polar, and aromatic residues, including W86 and Y108 (Figure 6). The SAR for the two series diverges at this point, and this placement would accommodate these differences. This pocket is just large enough to accommodate the C-4 substitutions off the aryl ring in the acyclic series and could provide favorable interactions for the aryl sulfonamide group, as well as hydrophobic interactions for the pyrrolidine series. Mutation of Y108 and W86 to alanine resulted in decreased affinities for all compounds that were tested (Table 1). A wide variety of 4-substituents off the piperidine ring is tolerated in both series. Therefore, the 4-substitution off the piperidine ring is docked heading out toward the extracellular portion of the model and near the loop connecting helix 4 to helix 5, ECL2 (Figure 6). The piperidine fits nicely in this channel with the 4-substitution going out toward the extracellular region of the receptor. This placement accommodates the bulky substituents, such as in compounds **1**−**3**, **6**, and **7** (Figure 7). Later in the program, a key polar site was identified off the 4-phenyl piperidine in both series. These polar groups could potentially interact with the polar residues in the extracellular loop, ECL2, or the nearby extracellular loop connecting helices 6 and 7, ECL3 (Figure 6). In bovine rhodopsin, ECL2 forms part of the chromophore-binding pocket. It is connected to the top of helix 3 with a disulfide bond that is conserved in many family A GPCRs, including the chemokines. This loop in CCR5 is similar in length to the loop in bovine rhodopsin (Figure 4), and one can postulate that it too would form part of the binding pocket. Previously, it has been shown that G163 is a critical site for binding and infectivity of R5 strains of HIV-1 for human CCR5 (*24*, *28*) and is predicted to lie at the juncture of TM4 and ECL2.

In conclusion, we have developed a CCR5 antagonist pharmacophore model based on the SAR from the 2-aryl-4-(piperidin-1-yl)butanamine and 1,3,4-trisubstituted pyrrolidine series and a receptor docking model which we have tested using site-directed mutagenesis experiments. Our results are consistent with a proposed binding site for the two series that is located within a cavity near the extracellular surface formed by transmembrane helices 2, 3, 6, and 7. This site is in a region similar to that for other proposed GPCR small molecule binding sites. It is partially overlapping the 11-*cis*-retinal binding site in the bovine rhodopsin crystal structure (*23*) and the proposed TAK-779 binding site (*17*).

ACKNOWLEDGMENT

We thank Ping Chen, Richard Budhu, and Bryan Oates for their synthetic assistance and Dr. Dennis Underwood for many insightful discussions at the beginning of this project.

REFERENCES

1. Choe, H., Farzan, M., Sun, Y., Sullivan, N., Rollins, B., Ponath, P. D., Wu, L., Mackay, C. R., LaRosa, G., Newman, W., Gerard, N., Gerard, C., and Sodroski, J. (1996) *Cell 85*, 1135−1148.
2. Doranz, B. J., Rucker, J., Yi, Y., Smyth, R. J., Samson, M., Peiper, S. C., Parmentier, M., Collman, R. G., and Doms, R. W. (1996) *Cell 85*, 1149−1158.

3. Dragic, T., Litwin, V., Allaway, G. P., Martin, S. R., Huang, Y., Nagashima, K. A., Cayanan, C., Maddon, P. J., Koup, R. A., Moore, J. P., and Paxton, W. A. (1996) *Nature 381*, 667.
4. Deng, H., Liu, R., Ellmeier, W., Choe, S., Unutmaz, D., Burkhart, M., Di Marzio, P., Marmon, S., Sutton, R. E., Hill, C. M., Davis, C. B., Peiper, S. C., Schall, T. J., Littman, D. R., and Landau, N. R. (1996) *Nature 381*, 661−666.
5. Alkhatib, G., Combadiere, C., Broder, C. C., Feng, Y., Kennedy, P. E., Murphy, P. M., and Berger, E. A. (1996) *Science 272*, 1955−1958.
6. Paxton, W. A., Martin, S. R., Tse, D., O'Brien, T. R., Skurnick, J., VanDevanter, N. L., Padian, N., Braun, J. F., Kotler, D. P., Wolinsky, S. M., and Koup, R. A. (1996) *Nat. Med. 2*, 412−417.
7. Liu, R., Paxton, W. A., Choe, S., Cerandini, D., Martin, S. R., Horuk, R., MacDonald, M. E., Stuhlmann, H., Koup, R. A., and Landau, N. R. (1996) *Cell 86*, 367−377.
8. Michael, N. L., Chang, G., Louie, L. G., Mascola, J. R., Dondero, D., Birx, D. L., and Sheppard, H. W. (1997) *Nat. Med. 3*, 338−340.
9. Cocchi, F., DeVico, A. L., Garzino-Demo, A., Arya, S. K., Gallo, R. C., and Lusso, P. (1995) *Science 270*, 1811−1815.
10. Baba, M., Nishimura, O., Kanzaki, N., Okamoto, M., Sawada, H., Iizawa, Y., Shiraishi, M., Aramaki, Y., Okonogi, K., Ogawa, Y., Mefuro, K., and Fujino, M. (1999) *Proc. Natl. Acad. Sci. U.S.A. 96*, 5698−5703.
11. Baroudy, B. (2000) Presented at the 7th Conference of Retroviruses and Opportunistic Infections, San Francisco, CA, Jan 31−Feb 3, Abstract S17.
12. Dorn, C. P., Finke, P. E., Oates, B., Budhu, R. J., Mills, S. G., MacCoss, M., Malkowitz, L., Springer, M. S., Daugherty, B. L., Gould, S. L., DeMartino, J. A., Siciliano, S. J., Carella, A., Carver, G., Holmes, K., Danzeisen, R., Hazuda, D., Kessler, J., Lineberger, J., Miller, M., Schlief, W. A., and Emini, E. A. (2001) *Bioorg. Med. Chem. Lett. 11*, 259−264.
13. Finke, P. E., Meurer, L. C., Oates, B., Mills, S. G., MacCoss, M., Malkowitz, L., Springer, M. S., Daugherty, B. L., Gould, S. L., DeMartino, J. A., Siciliano, S. J., Carella, A., Carver, G., Holmes, K., Danzeisen, R., Hazuda, D., Kessler, J., Lineberger, J., Miller, M., Schlief, W. A., and Emini, E. A. (2001) *Bioorg. Med. Chem. Lett. 11*, 265−270.
14. Finke, P. E., Meurer, L. C., Oates, B., Shah, S. K., Loebach, J. L., Mills, S. G., MacCoss, M., Castonguay, L., Malkowitz, L., Springer, M. S., Gould, S. L., and DeMartino, J. A. (2001) *Bioorg. Med. Chem. Lett. 11*, 2469−2473.
15. Hale, J. J., Budhu, R. J., Holson, E. B., Finke, P. E., Oates, B., Mills, S. G., MacCoss, M., Gould, S. L., DeMartino, J. A., Springer, M. S., Siciliano, S. J., Malkowitz, L. M., Schlief, W. A., Hazuda, D., Miller, M., Kessler, J., Danzeisen, R., Holmes, K., Lineberger, J., Carella, A., Carver, G., and Emini, E. A. (2001) *Bioorg. Med. Chem. Lett. 11*, 2741−2745.
16. Caldwell, C. G., Chen, P., Donnelly, K. F., Finke, P. E., Shankaran, K., Meurer, L. C., Oates, B., MacCoss, M., Mills, S. G., Malkowitz, L., Springer, M. S., Schlief, W. A., Carella, A., Carver, G., Holmes, K., and Emini, E. A. (2000) Presented at the American Chemical Society's 220th National Meeting, Washington, DC, Aug 20−25, Abstract MEDI-85.
17. Dragic, T., Trkola, A., Thompson, D. A. D., Cormier, E. G., Kajumo, F. A., Maxwell, E., Lin, S. W., Ying, W., Smith, S. O., Sakmar, T. P., and Moore, J. P. (2000) *Proc. Natl. Acad. Sci. U.S.A. 97*, 5639−5644.
18. Halgren, T. A. (1999) *J. Comput. Chem. 20*, 720−729.
19. Miller, M. D., Fluder, E. M., Castonguay, L. A., Culberson, J. C., Mosley, R. T., Prendergast, K., Kearsley, S. K., and Sheridan, R. P. (1999) *Med. Chem. Res. 9*, 513−534.
20. Quanta (2000) Accelrys, Inc., Burlington, MA.
21. Bernstein, F. C., Koetzle, T. F., Williams, G. J. B., Meyer, E. F., and Brice, M. D. (1977) *J. Mol. Biol. 112*, 535−542.
22. Brooks, B. B., Bruccoleri, R. E., Olafson, B. D., States, D. J., Swaminathan, S., and Karplus, M. (1983) *J. Comput. Chem. 4*, 187−217.
23. Palczewski, K., Kumasaka, T., Hori, T., Behnke, C. A., Motoshima, H., Fox, B. A., le Trong, I., Teller, D. C., Okada, T., Stenkamp, R. E., Yamamoto, M., and Miyano, M. (2000) *Science, 289*, 739−745.
24. Samson, M., Labbe, O., Mollereau, C., Vassart, G., and Parmentier, M. (1996) *Biochemistry 35*, 3362−3367.
25. Daugherty, B. L., and Springer, M. S. (1997) *Genomics 41*, 294−295.
26. Van Riper, G., Siciliano, S., Fischer, P. A., Meuer, R., Springer, M. S., and Rosen, H. (1993) *J. Exp. Med. 177*, 851−856.
27. Lynch, C. L., Gentry, A. L., Hale, J. J., Mills, S. G., MacCoss, M., Malkowitz, L., Springer, M. S., Gould, S. L., DeMartino, J. A., Siciliano, S. J., Cascieri, M. A., Doss, G., Carella, A., Carver, G., Holmes, K., Schleif, W. A., Danzeisen, R., Hazuda, D., Kessler, J., Lineberger, J., Miller, M., and Emini, E. A. (2002) *Bioorg. Med. Chem. Lett. 12*, 677−679.
28. Siciliano, S. J., Kuhmann, S. E., Weng, Y., Madani, N., Springer, M. S., Lineberger, J. E., Danzeisen, R., Miller, M. D., Kavanaugh, M. P., DeMartino, J. A., and Kabat, D. (1999) *J. Biol. Chem. 274*, 1905−1913.

BI026639S